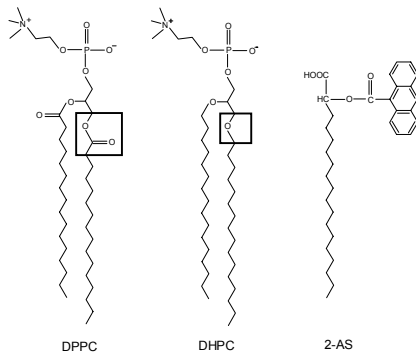


**Influence of Ester and Ether Linkage in Phospholipids on the Environment and Dynamics of the Membrane Interface: A Wavelength-Selective Fluorescence Approach**

Soumi Mukherjee and Amitabha Chattopadhyay

Langmuir; **2005**; 21(1) pp 287 - 293; (Research Article) DOI: [10.1021/la048027+](https://doi.org/10.1021/la048027+)



# Influence of Ester and Ether Linkage in Phospholipids on the Environment and Dynamics of the Membrane Interface: A Wavelength-Selective Fluorescence Approach

Soumi Mukherjee and Amitabha Chattopadhyay\*

Centre for Cellular and Molecular Biology, Uppal Road, Hyderabad 500 007, India

Received August 4, 2004. In Final Form: October 10, 2004

We have monitored the environment and dynamics of the membrane interface formed by the ester-linked phospholipid 1,2-dipalmitoyl-*sn*-glycero-3-phosphocholine (DPPC) and the ether-linked phospholipid 1,2-dihexadecyl-*sn*-glycero-3-phosphocholine (DHPC) utilizing the wavelength-selective fluorescence approach and using the fluorescent membrane probe 2-(9-anthroyloxy)stearic acid (2-AS). This interfacially localized probe offers a number of advantages over those which lack a fixed location in the membrane. When incorporated in membranes formed by DPPC and DHPC, 2-AS exhibits red edge excitation shift (REES) of 14 and 8 nm, respectively. This implies that the rate of solvent reorientation, as sensed by the interfacial anthroyloxy probe, in ester-linked DPPC membranes is slow compared to the rate of solvent reorientation in ether-linked DHPC membranes. In addition, the fluorescence polarization values of 2-AS are found to be higher in DHPC membranes than in DPPC membranes. This is further supported by wavelength-dependent changes in fluorescence polarization and lifetime. Taken together, these results are useful in understanding the role of interfacial chemistry on membrane physical properties.

## Introduction

Biological membranes are complex assemblies of lipids and proteins that allow cellular compartmentalization and act as the interface through which cells communicate with each other and with the external milieu. Organized molecular assemblies such as membranes can be considered as large cooperative units with characteristics very different from the individual structural units that constitute them. A direct consequence of such highly organized systems is the restriction imposed on the mobility of their constituent structural units.

Membranes exhibit a considerable degree of anisotropy along the axis perpendicular to the bilayer. This results in the anisotropic behavior of the constituent lipid molecules, and more importantly, the environment of a probe molecule becomes very much dependent on its precise localization in the membrane. While the center of the bilayer is nearly isotropic, the upper portion, only a few angstroms away toward the membrane surface, is highly ordered.<sup>1–6</sup> The membrane interface, the most important region as far as the dynamics and function of the membrane are concerned, is characterized by unique motional and dielectric characteristics<sup>2</sup> different from the bulk aqueous phase and the more isotropic hydrocarbon-like deeper regions of the membrane. This specific region of the membrane exhibits slow rates of solvent relaxation<sup>6</sup> and is known to participate in intermolecular charge interactions<sup>7</sup> and hydrogen bonding through the polar headgroup.<sup>8</sup>

The chemistry of the membrane interface can vary depending on the type of linkage (e.g., ester or ether) of the hydrocarbon chains to the glycerol backbone region.

This, in turn, could influence the organization and dynamics of the interface. Differences in organization in membranes of ester- and ether-linked phospholipids have earlier been detected by magnetic resonance, infrared spectroscopy, X-ray diffraction, monolayer studies, and differential scanning calorimetry.<sup>9–13</sup> In addition, the fluorescent membrane probe 6-propionyl-2-dimethylaminonaphthalene (PRODAN) and related derivatives have been used to monitor ester- and ether-linked phospholipid membranes.<sup>14–16</sup> However, PRODAN has no hydrophobic tail attached to it and therefore has a distribution of locations instead of a unique location when it partitions in the membrane. Interestingly, on the basis of hydrostatic pressure effects on its localization in the bilayer, it has previously been suggested that PRODAN binds to multiple sites of varying polarity in the membrane.<sup>17</sup> The choice of a suitable probe is thus of considerable importance in these studies. It is desirable that the chosen probe is able to intercalate with normal components of the membrane, that is, the phospholipids. For example, the membrane probe 6-palmitoyl-2-[[2-(trimethylammonio)ethyl]methylamino] naphthalene chloride (PATMAN) which has a fluorophore similar to PRODAN covalently attached to a hydrophobic tail can intercalate well with membrane phospholipids due to its fatty acyl chain.<sup>18,19</sup> Fatty acids labeled with fluorescent reporter groups have proved to be useful membrane probes. In particular, anthroyloxy

\* To whom all correspondence should be addressed. Phone: +91-40-2719-2578. Fax: +91-40-2716-0311. E-mail: amit@cceb.res.in.

(1) Seelig, J. *Q. Rev. Biophys.* **1977**, *10*, 353.  
 (2) Ashcroft, R. G.; Coster, H. G. L.; Smith, J. R. *Biochim. Biophys. Acta* **1981**, *643*, 191.  
 (3) Perochon, E.; Lopez, A.; Tocanne, J. F. *Biochemistry* **1992**, *31*, 7672.  
 (4) Venable, R. M.; Zhang, Y.; Hardy, B. J.; Pastor, R. W. *Science* **1993**, *262*, 223.  
 (5) Chattopadhyay, A.; Mukherjee, S. *Langmuir* **1999**, *15*, 2142.  
 (6) Chattopadhyay, A. *Chem. Phys. Lipids* **2003**, *122*, 3.

(7) Gennis, R. B. *Biomembranes: Molecular Structure and Function*; Springer-Verlag: New York, 1989.

(8) Boggs, J. M. *Biochim. Biophys. Acta* **1987**, *906*, 353.  
 (9) Ruocco, M. J.; Siminovich, D. J.; Griffin, R. G. *Biochemistry* **1985**, *24*, 2406.  
 (10) Kim, J. T.; Mattai, J.; Shipley, G. G. *Biochemistry* **1987**, *26*, 6592.  
 (11) Mattjus, P.; Bittman, R.; Slotte, J. P. *Langmuir* **1996**, *12*, 1284.  
 (12) Lewis, R. N. A. H.; Pohle, W.; McElhaney, R. N. *Biophys. J.* **1996**, *70*, 2746.  
 (13) Smaby, J. M.; Hermetter, A.; Schmid, P. C.; Paltauf, F.; Brockman, H. L. *Biochemistry* **1983**, *22*, 5808.  
 (14) Massey, J. B.; She, H. S.; Pownall, H. J. *Biochemistry* **1985**, *24*, 6973.  
 (15) Sommer, A.; Paltauf, F.; Hermetter, A. *Biochemistry* **1990**, *29*, 11134.  
 (16) Hutterer, R.; Schneider, F. W.; Hof, M. *J. Fluoresc.* **1997**, *7*, 27.  
 (17) Chong, L.-G. P. *Biochemistry* **1988**, *27*, 399.

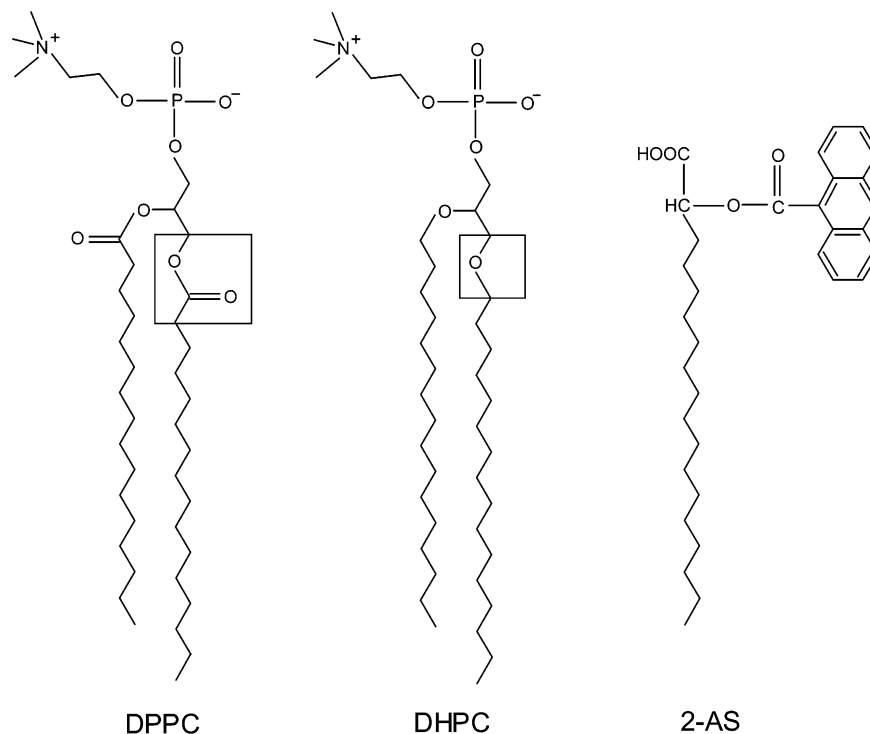


**Figure 1.** Chemical structures of the phospholipids (DPPC and DHPC) and the fluorescent membrane probe (2-AS) used. The ester and ether linkages in DPPC and DHPC are highlighted. The structure of 2-AS shown is the protonated form which is the predominant form under the experimental conditions (pH 5). See text for other details.

fatty acids such as 2-(9-anthroyloxy)stearic acid (2-AS) in which an anthracene group is attached by an ester linkage to an alkyl chain have been extensively used as fluorescent probes in membranes.<sup>5,20–24</sup> Depth analysis using the parallax method<sup>25</sup> has previously shown that the anthroyloxy group in 2-AS in its protonated form is localized at the membrane interface at a depth of 15.8 Å from the center of the membrane bilayer.<sup>21</sup> This is significant, since this location corresponds to the position of the carbonyls in bilayers formed by ester phospholipids.<sup>26</sup> In this paper, we have monitored the environment and dynamics of the membrane interface formed by ester- and ether-linked phospholipids (see Figure 1) utilizing the wavelength-selective fluorescence approach using 2-AS as the fluorescent probe.

Wavelength-selective fluorescence comprises a set of approaches based on the red edge effect in fluorescence spectroscopy which can be used to directly monitor the environment and dynamics around a fluorophore in an organized molecular assembly.<sup>6,27–29</sup> A shift in the wavelength of maximum fluorescence emission toward higher

wavelengths, caused by a shift in the excitation wavelength toward the red edge of the absorption band, is termed a red edge excitation shift (REES). This effect is mostly observed with polar fluorophores in motionally restricted media such as very viscous solutions or condensed phases where the dipolar relaxation time for the solvent shell around a fluorophore is comparable to or longer than its fluorescence lifetime. This approach allows the mobility parameters of the environment itself (i.e., dynamics of solvation which is represented by the relaxing solvent molecules) to be probed using the fluorophore merely as a reporter group. The unique feature of REES is that, while other fluorescence techniques yield information about the fluorophore itself, REES provides information about the relative rates of solvent relaxation which is not possible to obtain by other techniques. We have previously shown that REES and related techniques (the wavelength-selective fluorescence approach) serve as powerful tools for monitoring the organization and dynamics of probes and peptides bound to membranes<sup>5,20,30–34</sup> and membrane-mimetic media such as micelles<sup>35–37</sup> and reverse micelles.<sup>38–40</sup> Utilizing this approach, we show here the differences in

(18) Lakowicz, J. R.; Bevan, D. R.; Maliwal, B. P.; Cherek, H.; Balter, A. *Biochemistry* **1983**, *22*, 5714.

(19) Sykora, J.; Kapusta, P.; Fidler, V.; Hof, M. *Langmuir* **2002**, *18*, 571.

(20) Kelkar, D. A.; Ghosh, A.; Chattopadhyay, A. *J. Fluoresc.* **2003**, *13*, 459.

(21) Abrams, F. S.; Chattopadhyay, A.; London, E. *Biochemistry* **1992**, *31*, 5322.

(22) Thulborn, K. R.; Sawyer, W. H. *Biochim. Biophys. Acta* **1978**, *511*, 125.

(23) Villain, J.; Prieto, M. *Chem. Phys. Lipids* **1991**, *59*, 9.

(24) Hutterer, R.; Schneider, F. W.; Lanig, H.; Hof, M. *Biochim. Biophys. Acta* **1997**, *1323*, 195.

(25) Chattopadhyay, A.; London, E. *Biochemistry* **1987**, *26*, 39.

(26) White, S. H.; Wimley, W. C. *Curr. Opin. Struct. Biol.* **1994**, *4*, 79.

(27) Mukherjee, S.; Chattopadhyay, A. *J. Fluoresc.* **1995**, *5*, 237 and references therein.

(28) Raghuraman, H.; Kelkar, D. A.; Chattopadhyay, A. *Proc. Indian Natl. Sci. Acad., Part A* **2003**, *69*, 25.

(29) Demchenko, A. P. *Luminescence* **2002**, *17*, 19.

(30) Chattopadhyay, A.; Mukherjee, S. *Biochemistry* **1993**, *32*, 3804.

(31) Ghosh, A. K.; Rukmini, R.; Chattopadhyay, A. *Biochemistry* **1997**, *36*, 14291.

(32) Chattopadhyay, A.; Mukherjee, S. *J. Phys. Chem. B* **1999**, *103*, 8180.

(33) Mukherjee, S.; Raghuraman, H.; Dasgupta, S.; Chattopadhyay, A. *Chem. Phys. Lipids* **2004**, *127*, 91.

(34) Rawat, S. S.; Kelkar, D. A.; Chattopadhyay, A. *Biophys. J.* **2004**, *87*, 831.

(35) Rawat, S. S.; Mukherjee, S.; Chattopadhyay, A. *J. Phys. Chem. B* **1997**, *101*, 1922.

(36) Raghuraman, H.; Pradhan, S. K.; Chattopadhyay, A. *J. Phys. Chem. B* **2004**, *108*, 2489.

(37) Raghuraman, H.; Chattopadhyay, A. *Eur. Biophys. J.* **2004**, *33*, 611.

(38) Chattopadhyay, A.; Mukherjee, S.; Raghuraman, H. *J. Phys. Chem. B* **2002**, *106*, 13002.

(39) Raghuraman, H.; Chattopadhyay, A. *Langmuir* **2003**, *19*, 10332.

interfacial dynamics in membranes of ester- and ether-linked phospholipids.

### Experimental Section

**Materials.** 1,2-dipalmitoyl-*sn*-glycero-3-phosphocholine (DPPC) and 1,2-dihexadecyl-*sn*-glycero-3-phosphocholine (DHPC) were obtained from Avanti Polar Lipids (Alabaster, AL). 1,2-dimyristoyl-*sn*-glycero-3-phosphocholine (DMPC) was purchased from Sigma Chemical Co. (St. Louis, MO). 2-AS was purchased from Molecular Probes (Eugene, OR). Lipids were checked for purity by thin-layer chromatography on precoated silica gel plates (Sigma) in chloroform/methanol/water (65:35:5, v/v/v) and were found to give only one spot in all cases with a phosphate-sensitive spray and on subsequent charring.<sup>41</sup> The concentrations of stock solutions of phospholipids were determined by phosphate assay after total digestion by perchloric acid using Na<sub>2</sub>HPO<sub>4</sub> as a standard.<sup>42</sup> DMPC was used as an internal standard to assess lipid digestion. Concentrations of stock solutions of 2-AS in methanol were estimated using a molar extinction coefficient ( $\epsilon$ ) of 8000 M<sup>-1</sup> cm<sup>-1</sup> at 361 nm.<sup>43</sup> All other chemicals used were of the highest purity available. The solvents used were of spectroscopic grade. Water was purified through a Millipore (Bedford, MA) Milli-Q system and used throughout.

**Preparation of Vesicles.** All experiments were conducted using large unilamellar vesicles (LUVs) of 100 nm diameter containing 1 mol % 2-AS. In general, 320 nmol of lipid (DPPC or DHPC) in methanol was mixed with 3.2 nmol of 2-AS in methanol. The sample was mixed well and dried under a stream of nitrogen while being warmed gently (~35 °C). After further drying under a high vacuum for at least 6 h, 1.5 mL of 10 mM sodium acetate, 150 mM sodium chloride, and pH 5.0 buffer was added and the lipid samples were hydrated (swelled) well above the phase transition temperature of the phospholipid used while being intermittently vortexed for 3 min to disperse the lipid and form homogeneous multilamellar vesicles (MLVs). The lipid suspensions were maintained at ~60 °C (i.e., above the phase transition temperature) as the vesicles were made. LUVs with a diameter of 100 nm were prepared by the extrusion technique using an Avestin Liposofast extruder (Ottawa, Ontario, Canada) as previously described.<sup>44</sup> Briefly, the multilamellar vesicles were freeze-thawed five times by cycling in liquid nitrogen and water maintained at 60 °C to ensure solute equilibration between trapped and bulk solutions and then extruded through polycarbonate filters (pore diameter of 100 nm) mounted in the extruder fitted with Hamilton syringes (Hamilton Company, Reno, NV). The samples were subjected to 11 passes through the polycarbonate filter to give the final LUV suspension. The samples were incubated in the dark for 12 h at room temperature (23 °C) for equilibration before measuring fluorescence. Background samples were prepared in the same way except that fluorophore was not added to them. All experiments were performed at room temperature (23 °C) where DPPC and DHPC membranes are in the gel phase.

**Steady-State Fluorescence Measurements.** Steady-state fluorescence measurements were performed with a Hitachi F-4010 spectrofluorometer using 1 cm path length quartz cuvettes. Excitation and emission slits with a nominal band-pass of 5 nm were used for all measurements. The background intensities of samples in which 2-AS was omitted were negligible in most cases and were subtracted from each sample spectrum to cancel out any contribution due to the solvent Raman peak and other scattering artifacts. The spectral shifts obtained with different sets of samples were identical in most cases. In other cases, the values were within  $\pm 1$  nm of the ones reported. Fluorescence polarization measurements were performed using a Hitachi polarization accessory. Polarization values were calculated from the following equation:<sup>45</sup>

$$P = \frac{I_{VV} - GI_{VH}}{I_{VV} + GI_{VH}} \quad (1)$$

where  $I_{VV}$  and  $I_{VH}$  are the measured fluorescence intensities (after

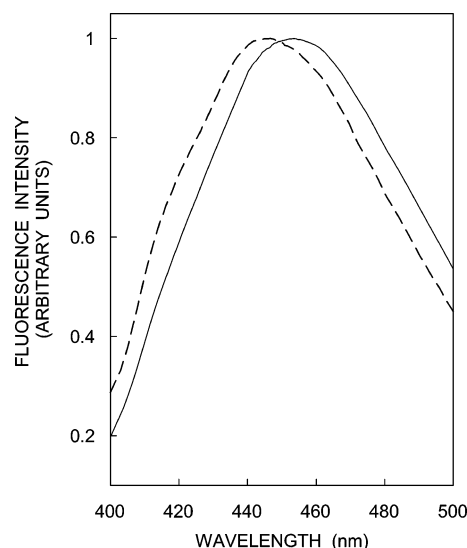


**Figure 2.** Fluorescence emission spectra of 2-AS in LUVs of DPPC (---) and DHPC (—). The lipid concentration was 0.21 mM, and the probe-to-lipid ratio was 1:100 (mol/mol). The spectra are intensity-normalized at the emission maximum. The excitation wavelength was 365 nm in both cases. See the Experimental Section for other details.

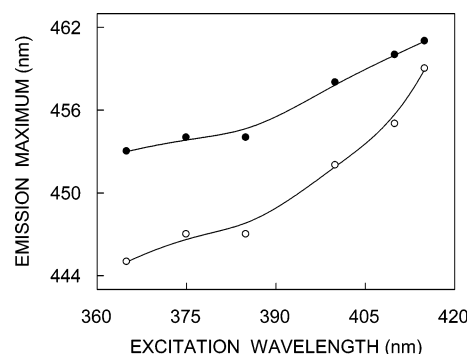


**Figure 3.** Effect of changing the excitation wavelength on the wavelength of maximum emission for 2-AS in LUVs of DPPC (○) and DHPC (●). All other conditions are the same as those in Figure 2. See the Experimental Section for other details.

appropriate background subtraction) with the excitation polarizer vertically oriented and the emission polarizer vertically and horizontally oriented, respectively.  $G$  is the grating correction factor and is the ratio of the efficiencies of the detection system for vertically and horizontally polarized light, and it is equal to  $I_{HV}/I_{HH}$ . All experiments were done with multiple sets of samples, and average values of polarization are shown in Figure 6.

**Time-Resolved Fluorescence Measurements.** Fluorescence lifetimes were calculated from time-resolved fluorescence intensity decays using a Photon Technology International (London, Western Ontario, Canada) LS-100 luminescence spectrophotometer in the time-correlated single photon counting mode. This machine uses a thyatron-gated nanosecond flash lamp filled with nitrogen as the plasma gas (16  $\pm$  1 in. of mercury vacuum) and is run at 17–22 kHz. Lamp profiles were measured at the excitation wavelength using Ludox (colloidal silica) as the scatterer. To optimize the signal-to-noise ratio, 10 000 photon counts were collected in the peak channel. All experiments were performed using excitation and emission slits with a nominal band-pass of 4 nm or less. The sample and the scatterer were alternated after every 5% (i.e., after 500 counts were collected

(41) Dittmer, J. C.; Lester, R. L. *J. Lipid. Res.* **1964**, *5*, 126.

(42) McClare, C. W. F. *Anal. Biochem.* **1971**, *39*, 527.

(43) Haugland, R. P. *Handbook of Fluorescent Probes and Research Chemicals*, 6th ed.; Molecular Probes: Eugene, OR, 1996.

(44) MacDonald, R. C.; MacDonald, R. I.; Menco, B. P.; Takeshita, K.; Subbarao, N. K.; Hu, L. R. *Biochim. Biophys. Acta* **1991**, *1061*, 297.

(45) Lakowicz, J. R. *Principles of Fluorescence Spectroscopy*; Plenum Press: New York, 1999.

(40) Kelkar, D. A.; Chattopadhyay, A. *J. Phys. Chem. B* **2004**, *108*, 12151.

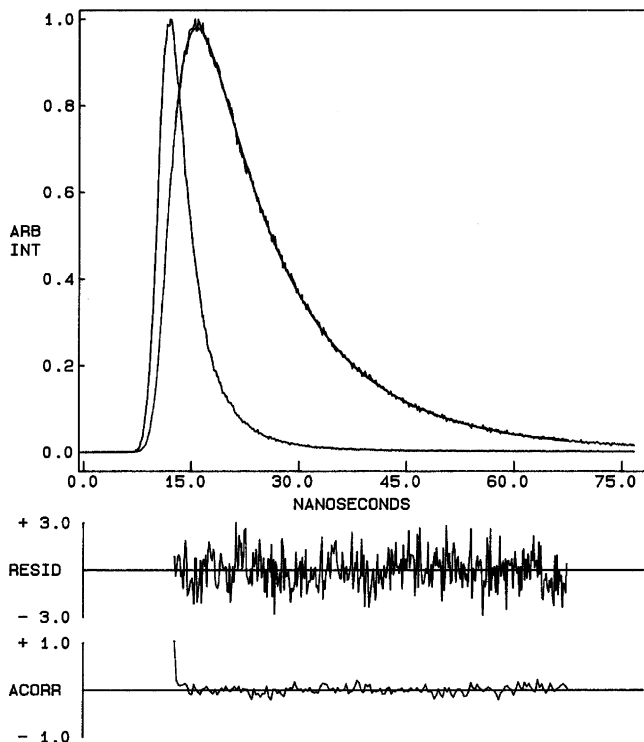


**Figure 4.** Time-resolved fluorescence intensity decay of 2-AS in DPPC LUVs. The excitation wavelength was 365 nm, and emission was monitored at 440 nm. The sharp peak on the left is the lamp profile. The relatively broad peak on the right is the decay profile, fitted to a biexponential function. The two lower plots show the weighted residuals and the autocorrelation function of the weighted residuals. All other conditions are the same as those in Figure 2. See the Experimental Section for other details.

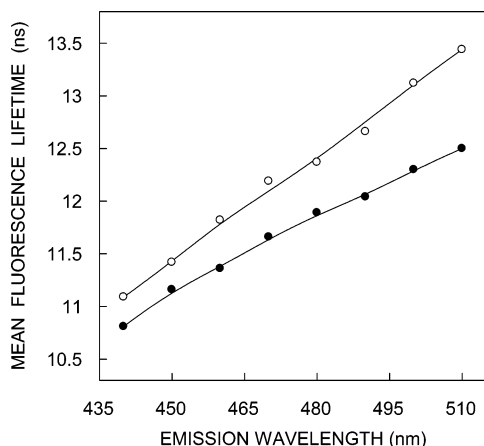


**Figure 5.** Mean fluorescence lifetime of 2-AS in DPPC (○) and DHPC (●) LUVs as a function of emission wavelength. The excitation wavelength was 365 nm. The mean fluorescence lifetimes were calculated from Table 1 using eq 3. All other conditions are the same as those in Figure 2. See Experimental Section for other details.

each time) acquisition to ensure compensation for shape and timing drifts occurring during the period of data collection.<sup>46</sup> This arrangement also prevents any prolonged exposure of the sample to the excitation beam, thereby avoiding any possible photodamage of the fluorophore. The data stored in a multi-channel analyzer was routinely transferred to an IBM PC for analysis. The fluorescence intensity decay curves so obtained were deconvoluted with the instrument response function and

(46) Bevington, P. R. *Data Reduction and Error Analysis for the Physical Sciences*; McGraw-Hill: New York, 1969.

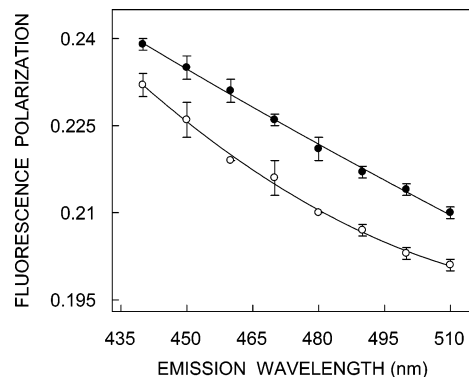


**Figure 6.** Fluorescence polarization of 2-AS in DPPC (○) and DHPC (●) LUVs as a function of emission wavelength. The excitation wavelength was 365 nm in both cases. All other conditions are the same as those in Figure 2. The data points shown are the means  $\pm$  standard errors of at least six independent measurements. See the Experimental Section for other details.

analyzed as a sum of exponential terms:

$$F(t) = \sum_i \alpha_i \exp(-t/\tau_i) \quad (2)$$

where  $F(t)$  is the fluorescence intensity at time  $t$  and  $\alpha_i$  is a preexponential factor representing the fractional contribution to the time-resolved decay of the component with a lifetime ( $\tau_i$ ) such that  $\sum_i \alpha_i = 1$ . The decay parameters were recovered using a nonlinear least squares iterative fitting procedure based on the Marquardt algorithm.<sup>46</sup> The program also includes statistical and plotting subroutine packages.<sup>47</sup> The goodness of the fit of a given set of observed data and the chosen function was evaluated by the reduced  $\chi^2$  ratio, the weighted residuals,<sup>48</sup> and the autocorrelation function of the weighted residuals.<sup>49</sup> A fit was considered acceptable when plots of the weighted residuals and the autocorrelation function showed random deviation about zero with a minimum  $\chi^2$  value of no more than 1.4. Mean (average) lifetimes ( $\langle\tau\rangle$ ) for biexponential decays of fluorescence were calculated from the decay times and preexponential factors using the following equation:<sup>45</sup>

$$\langle\tau\rangle = \frac{\alpha_1\tau_1^2 + \alpha_2\tau_2^2}{\alpha_1\tau_1 + \alpha_2\tau_2} \quad (3)$$

## Results

Figure 1 shows the chemical structures of the ester- and ether-linked phospholipids (DPPC and DHPC) used in this study. Their structures are identical except for the type of linkage of the hydrocarbon chains to the glycerol backbone. Thus, both DPPC and DHPC have saturated 16-carbon-atom chains as hydrocarbon tails and phosphatidylcholine as the headgroup. The only difference is that, while DPPC has an ester linkage, DHPC has an ether linkage in its structure. Figure 1 also shows the structure of 2-AS, the fluorescent probe used in which the fluorescent anthroyloxy group has been shown to be localized at the membrane interface.<sup>5,21–24</sup>

Our goal was to explore the change in organization and dynamics of a membrane-bound fluorescent probe when the interfacial chemistry of the phospholipid constituting the host membrane is changed from ester- to ether-type linkage. Ideally, this should be accompanied by minimal change in the chemical structure of the host lipids, a

(47) O'Connor, D. V.; Phillips, D. *Time-Correlated Single Photon Counting*; Academic Press: London, 1984; pp 180–189.

(48) Lampert, R. A.; Chewter, L. A.; Phillips, D.; O'Connor, D. V.; Roberts, A. J.; Meech, S. R. *Anal. Chem.* **1983**, *55*, 68.

(49) Grinvald, A.; Steinberg, I. Z. *Anal. Biochem.* **1974**, *59*, 583.

requirement that is fulfilled by DPPC and DHPC, since they differ only by their interfacial chemistry (i.e., ester vs ether linkage). An important criterion for the choice of an appropriate fluorescent probe, especially for studies using the wavelength-selective fluorescence approach, is a unique location of the probe in the membrane.<sup>30</sup> This is met by 2-AS, since its orientation and location in the membrane is known.<sup>5,21–24</sup> In addition, since the  $pK_a$  of membrane-bound 2-AS is  $\sim 7$ ,<sup>50</sup> we chose a pH of 5 for all of our measurements so that the carboxyl group in 2-AS is in its protonated state which is electrically neutral<sup>21</sup> (see Figure 1). Importantly, this also avoids any ground-state heterogeneity due to ionization of the carboxyl group.<sup>21</sup>

The fluorescence emission spectra for 2-AS in DPPC and DHPC vesicles in the gel phase are shown in Figure 2. The emission maximum<sup>51</sup> of 2-AS in DPPC LUVs is found to be at 445 nm. The emission maximum displays a red shift of 8 nm in DHPC vesicles and is at 453 nm. This indicates that the fluorescent anthroxyloxy group experiences a more polar environment in DHPC membranes probably due to the greater water penetration in ether-linked phospholipid membranes as reported earlier.<sup>12–15</sup> The shifts in the maxima of fluorescence emission of 2-AS in DPPC and DHPC vesicles as a function of excitation wavelength are shown in Figure 3. As the excitation wavelength is changed from 365 to 415 nm, the emission maximum of 2-AS in DPPC vesicles shifts from 445 to 459 nm, which corresponds to a REES of 14 nm. Such a shift in the wavelength of the emission maximum with a change in the excitation wavelength is characteristic of REES and indicates that the anthroxyloxy moiety in 2-AS is localized in a motionally restricted region of the DPPC membrane that offers considerable resistance to solvent reorientation in the excited state.<sup>5</sup> Interestingly, the emission maximum of 2-AS in DHPC membranes shows a reduction in REES in the same range of excitation wavelength. The emission maximum of 2-AS in DHPC vesicles shifts from 453 to 461 nm as the excitation wavelength is changed from 365 to 415 nm, which amounts to a REES of 8 nm. These results show that the magnitude of REES obtained for the same interfacial probe 2-AS varies with the chemical nature of the linkage in the phospholipid. We attribute this to the change in the microenvironment experienced by the probe in these two cases induced by the change in interfacial chemistry of the two phospholipids. In other words, the rate of solvent reorientation, as sensed by the interfacial anthroxyloxy probe, in DPPC membranes appears to be slow compared to the rate of solvent reorientation in DHPC membranes. It has been reported earlier using PRODAN that the rate of solvent reorientation is slower in fluid phase membranes of ester-linked phospholipids than the rate observed in membranes of ether-linked phospholipids.<sup>15</sup> Our results suggest this to be true even in the case of gel phase membranes for probes such as 2-AS which are localized at the interfacial region of the membrane.

REES originates from differential extents of solvent reorientation around the excited-state fluorophore, with each excitation wavelength selectively exciting a different

**Table 1. Lifetimes of 2-AS as a Function of Emission Wavelength<sup>a</sup>**

| emission wavelength (nm) | $\alpha_1$ | $\tau_1$ (ns) | $\alpha_2$ | $\tau_2$ (ns) |
|--------------------------|------------|---------------|------------|---------------|
| DPPC                     |            |               |            |               |
| 440                      | 0.43       | 4.81          | 0.57       | 12.86         |
| 450                      | 0.44       | 5.36          | 0.56       | 13.33         |
| 460                      | 0.40       | 5.57          | 0.60       | 13.53         |
| 470                      | 0.39       | 6.27          | 0.61       | 13.90         |
| 480                      | 0.36       | 7.32          | 0.64       | 13.87         |
| 490                      | 0.43       | 8.22          | 0.57       | 14.55         |
| 500                      | 0.72       | 10.62         | 0.28       | 17.12         |
| 510                      | 0.82       | 11.59         | 0.18       | 18.68         |
| DHPC                     |            |               |            |               |
| 440                      | 0.44       | 4.92          | 0.56       | 12.62         |
| 450                      | 0.43       | 5.88          | 0.57       | 12.97         |
| 460                      | 0.34       | 5.00          | 0.66       | 12.65         |
| 470                      | 0.38       | 6.70          | 0.62       | 13.20         |
| 480                      | 0.35       | 7.16          | 0.65       | 13.26         |
| 490                      | 0.39       | 8.52          | 0.61       | 13.47         |
| 500                      | 0.40       | 8.62          | 0.60       | 13.83         |
| 510                      | 0.89       | 11.16         | 0.11       | 18.89         |

<sup>a</sup> Excitation wavelength of 365 nm.

average population of fluorophores.<sup>27</sup> Since fluorescence lifetime serves as a faithful indicator for the local environment of a given fluorophore<sup>52</sup> and is sensitive to excited-state reactions, differential extents of solvent relaxation around a given fluorophore in the excited-state could be expected to give rise to differences in its fluorescence lifetime. In addition, the fluorescence lifetime of 2-AS is known to be sensitive to the solvent polarity and the environment in which it is placed and is known to be reduced as the polarity of the environment is increased.<sup>53,54</sup> A typical intensity decay profile of 2-AS incorporated into DPPC vesicles with its biexponential fitting and the various statistical parameters used to check the goodness of the fit is shown in Figure 4. Table 1 shows the fluorescence lifetimes of 2-AS in DPPC and DHPC membranes as a function of emission wavelength, keeping the excitation wavelength constant at 365 nm. All fluorescence decays could be fitted well with a biexponential function. We chose to use the mean fluorescence lifetime as an important parameter for describing the behavior of 2-AS in these membranes, since it is independent of the number of exponentials used to fit the time-resolved fluorescence decay. The mean fluorescence lifetimes were calculated from Table 1 using eq 3 and are plotted as a function of emission wavelength in Figure 5. The lifetimes of 2-AS in DHPC vesicles appear to be shorter than the lifetimes in DPPC vesicles. This could be due to a relatively polar environment experienced by the anthroxyloxy group in DHPC membranes due to greater water penetration<sup>12–15</sup> and the dependence of the fluorescence lifetime of 2-AS on solvent polarity.<sup>53,54</sup> Interestingly, the lifetime shows a considerable increase with increasing emission wavelength from 440 to 510 nm for both DPPC and DHPC membranes. Similar observation of increasing lifetime with increasing emission wavelength has previously been reported for fluorophores in environments of restricted mobilities.<sup>27</sup> Such increasing lifetimes across the emission spectrum may be interpreted in terms of solvent reorientation around the excited-state fluorophore as follows. Observation of emission spectra at shorter

(50) Von Tscharnner, V.; Radda, G. K. *Biochim. Biophys. Acta* **1981**, *643*, 435.

(51) We have used the term maximum of fluorescence emission in a somewhat wider sense here. In every case, we have monitored the wavelength corresponding to maximum fluorescence intensity as well as the center of mass of the fluorescence emission. In most cases, both these methods yielded the same wavelength. In cases where minor discrepancies were found, the center of mass of emission has been reported as the fluorescence maximum.

(52) Prendergast, F. G. *Curr. Opin. Struct. Biol.* **1991**, *1*, 1054.

(53) Thulborn, K. R.; Tilley, L. M.; Sawyer, W. H.; Treloar, F. E. *Biochim. Biophys. Acta* **1979**, *558*, 166.

(54) Garrison, M. D.; Doh, L. M.; Potts, R. O.; Abraham, W. *Chem. Phys. Lipids* **1994**, *70*, 155.

wavelengths selects for predominantly unrelaxed fluorophores. Their lifetimes are shorter because this population is decaying both at the rate of fluorescence emission at the given excitation wavelength and by decay to longer (unobserved) wavelengths. In contrast, observation at the long wavelength (red edge) of the emission selects for the more relaxed fluorophores, which have spent enough time in the excited state to allow increasingly larger extents of solvent relaxations.

These longer-lived fluorophores, which emit at higher wavelengths, should have more time to rotate in the excited state, giving rise to lower polarization. Figure 6 shows the variation in fluorescence polarization of 2-AS in DPPC and DHPC membranes as a function of emission wavelength, keeping the excitation wavelength constant at 365 nm. As seen from the figure, there is a considerable decrease in the polarization of 2-AS in both cases with increasing emission wavelength. The lowest polarization is observed toward longer wavelengths (red edge) where emission from the relaxed fluorophores predominates. Similar observations have previously been reported for other fluorophores in environments of restricted mobility.<sup>27</sup> Interestingly, the polarization values of 2-AS in general are found to be higher in DHPC membranes than in DPPC membranes. The higher value for polarization could be reflective of the interdigitation in DHPC membranes<sup>9</sup> which has earlier been shown to increase polarization.<sup>55</sup>

To ensure that the observed changes in the steady-state polarization of 2-AS in DPPC and DHPC membranes (Figure 6) are not due to any change in lifetimes (see Table 1 and Figure 5), the apparent (average) rotational correlation times for 2-AS were calculated using Perrin's equation:<sup>45</sup>

$$\tau_c = \frac{\langle \tau \rangle r}{r_0 - r} \quad (4)$$

where  $r_0$  is the limiting anisotropy of the anthroyloxy probe and  $\langle \tau \rangle$  is the mean fluorescence lifetime as calculated from eq 3. Although Perrin's equation is not strictly applicable here, its use as a first approximation is justified, since we have used mean fluorescence lifetimes for the analysis of multiple component lifetimes. The values of the apparent rotational correlation times, calculated this way using a value of  $r_0$  of 0.275 corresponding to an excitation wavelength of 365 nm,<sup>56</sup> are shown in Figure 7 as a function of emission wavelength. The apparent rotational correlation times of 2-AS in DPPC and DHPC membranes show a continuous reduction with increasing emission wavelength which supports the polarization data (Figure 6) and indicates that the rotational mobility of the probe increases with increasing emission wavelength. Importantly, the overall trend in the change in apparent rotational correlation times with emission wavelength parallels the observed change in polarization. This ensures that the observed change in polarization values is free from lifetime-induced artifacts. However, the decrease in steady-state polarization with increasing wavelength (Figure 6) could also be rationalized by the emission wavelength-dependent intramolecular rotational relaxation of the anthroyloxy group.<sup>57–59</sup>

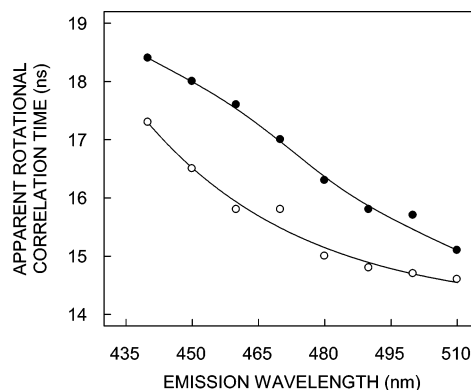


**Figure 7.** Apparent rotational correlation times of 2-AS in DPPC (○) and DHPC (●) LUVs as a function of emission wavelength. The excitation wavelength was 365 nm, and the apparent rotational correlation times were calculated using eq 4. All other conditions are the same as those in Figure 2. See text for other details.

## Discussion

The wavelength-selective fluorescence approach represents a powerful and sensitive tool for studying membrane organization and dynamics.<sup>6,27</sup> We have previously reported changes in membrane dynamics detected using this approach due to changes in probe location as a function of the membrane penetration depth,<sup>5</sup> phase state of the membrane,<sup>32</sup> ionization state,<sup>33</sup> and charge of the lipid headgroup.<sup>20</sup> This report is focused on monitoring the environment and dynamics of the membrane interface formed by ester- and ether-linked phospholipids utilizing the wavelength-selective fluorescence approach using 2-AS as a suitable fluorescent membrane probe. The probe 2-AS is an appropriate choice for wavelength-selective fluorescence studies, since it exhibits a large change in dipole moment (4.5 D) upon excitation,<sup>57</sup> an important criterion for displaying REES.<sup>6,27</sup> In addition, the anthroyloxy group in 2-AS is localized at the membrane interface,<sup>20</sup> the most sensitive region in the membrane for displaying REES and wavelength-selective fluorescence effects.<sup>6</sup> Interestingly, it has recently been shown that 2-AS and PATMAN monitor similar regions in the membrane bilayer in the fluid phase.<sup>19</sup>

The conformational and structural differences between ester and ether phospholipids are manifestations of the replacement of the ester  $sp^2$  carbon of the carbonyl group with a  $sp^3$  carbon of the ether linkage.<sup>9</sup> The additional water molecules from increased hydration in ether phospholipids<sup>12–15</sup> may replace the space occupied by the carbonyl groups in ester phospholipids.<sup>14</sup> In addition, ether phospholipids lack carbonyl groups at the site of attachment to the glycerol backbone. As a consequence, there is reduced hydrogen bonding between ether phospholipids which allows tighter packing of the hydrocarbon chains which results in a small increase in the transition enthalpy and temperature.<sup>60</sup> The tighter packing of the hydrocarbon chains could give rise to higher polarization in ether phospholipids (Figure 6).

Our results show that the rate of solvent reorientation, as sensed by the interfacial anthroyloxy probe, in ester-linked DPPC membranes is slow compared to the rate of solvent reorientation in ether-linked DHPC membranes. The slower rate of solvent relaxation in DPPC membranes could be attributed to the hydrogen-bonded water at the carbonyl group of ester lipids.<sup>13</sup> This results in significantly

(55) Hutterer, R.; Schneider, F. W.; Hof, M. *Chem. Phys. Lipids* **1997**, *86*, 51.

(56) Vincent, M.; de Foresta, B.; Gallay, J.; Alfsen, A. *Biochemistry* **1982**, *21*, 708.

(57) Werner, T. C.; Hoffman, R. M. *J. Phys. Chem.* **1973**, *77*, 1611.

(58) Matayoshi, E. D.; Kleinfeld, A. M. *Biophys. J.* **1981**, *35*, 215.

(59) Berberan-Santos, M. N.; Prieto, M. J. E.; Szabo, A. G. *J. Phys. Chem.* **1991**, *95*, 5471.

(60) McKeone, B. J.; Pownall, H. J.; Massey, J. B. *Biochemistry* **1986**, *25*, 7711.

different dielectric properties at the interfacial region of membranes formed by ester and ether lipids. This difference in dielectric (dipolar) environment in the two cases could influence REES. We have used gel phase membranes in our study, since the structural and organizational differences between DPPC and DHPC membranes are enhanced in the gel phase.<sup>10,61</sup> Another contribution to differential REES effects in these cases could be from the dipole potential of the membranes. The dipole potential of a membrane is a manifestation of a nonrandom orientation of constitutive and adsorbed electric dipoles in the lipid-water interface (i.e., dipoles of lipid headgroups, the interfacial region, and the membrane-associated water molecules).<sup>62</sup> Interestingly, the polarity of the carbonyl group in ester lipids has been reported to be responsible for the larger dipole potential for DPPC compared to the value for DHPC.<sup>61</sup>

In summary, our results show that there is a significant change in the dynamics of the membrane interfacial region when the chemistry of the membrane interface is changed.

---

(61) Gawrisch, K.; Ruston, D.; Zimmerberg, J.; Parsegian, V. A.; Rand, R. P.; Fuller, N. *Biophys. J.* **1992**, *61*, 1213.

These results are relevant, since ether-linked phospholipids are functionally important lipids found in halophilic bacteria, cardiac tissue, and the central nervous system.<sup>63</sup> The physicochemical properties of membranes formed by ether lipids will play an important role in membrane processes such as interaction with proteins which in turn will affect membrane function. The altered interfacial characteristics of these membranes reported here could be useful in understanding their role in natural membranes.

**Acknowledgment.** This work was supported by the Council of Scientific and Industrial Research, Government of India. We thank Y. S. S. V. Prasad and G. G. Kingi for technical help and members of our laboratory for critically reading the manuscript. S.M. thanks the Council of Scientific and Industrial Research for the award of a Senior Research Fellowship.

LA048027+

---

(62) Brockman, H. *Chem. Phys. Lipids* **1994**, *73*, 57.

(63) Paltauf, F. *Chem. Phys. Lipids* **1994**, *74*, 101.